

Cite this: *Phys. Chem. Chem. Phys.*, 2012, **14**, 482–494

www.rsc.org/pccp

PAPER

Statistical thermodynamics of the isomerization reaction between *n*-heptane and isoheptane†

Tao Yu, Jingjing Zheng and Donald G. Truhlar*

Received 11th August 2011, Accepted 21st September 2011

DOI: 10.1039/c1cp22578b

We have employed electronic structure calculations and the recently proposed multi-structural (MS) anharmonicity method to calculate partition functions and thermodynamic quantities, in particular entropy and heat capacity, for *n*-heptane and isoheptane. We included all structures, of which there are 59 for *n*-heptane and 37 for isoheptane, and we carried out the calculations both in the local harmonic approximation and by including torsional (T) anharmonicity. In addition, ΔS° , ΔH , and ΔG° for the isomerization reaction between these two species were also calculated. It is found that all calculated thermodynamic quantities based on the MS-T approximation in the temperature range from 298 K to 1500 K agree well with experimental data from the American Petroleum Institute (API) tables or Thermodynamics Research Center (TRC) data series and with values obtained from Benson's empirical parameters fit to experiment. This demonstrates not only the high accuracy of the electronic structure calculations but also that the MS-T method can be used to include both multiple-structure anharmonicity and torsional anharmonicity in the calculation of thermodynamic properties for complex molecules that contain many torsions. It also gives us confidence that we can apply the MS-T statistical thermodynamic method to obtain thermodynamic properties (i) over a broader temperature range than that for which data are available in the API tables, TRC data series, or from empirical estimation and (ii) to the many molecules for which experimental data are not available at any temperature.

Introduction

The thermodynamic properties of molecules are important in almost all branches of chemistry and chemical engineering. Thermodynamic data (or, for transition states, quasi-thermodynamic data), such as entropy, enthalpy, and Gibbs free energy, are required to calculate heats of reaction, chemical equilibrium constants, and thermal reaction rate constants. This kind of data can be determined by either experimental measurements or statistical mechanical computations. The example to be considered here is the determination of the thermodynamic properties of alkanes; such data are needed for, among other uses, understanding combustion and pyrolysis mechanisms.

Thermodynamic properties of alkanes in the gas phase can be obtained by three approaches, namely (i) direct experimental measurements, (ii) empirical estimations based on experiments on related systems, possibly combined with experiments on the

same system under different conditions, and (iii) electronic structure calculations combined with statistical mechanics. In approaches (i) and (ii) one can distinguish approaches involving direct measurements of thermodynamic properties such as heats of reaction and heat capacities (methods of type i-a and ii-a) and approaches based on measurement of spectroscopic properties from which thermodynamic variables may be inferred by statistical mechanics (methods of type i-b and ii-b); thermodynamic tables are often constructed using a combination of methods of all four types. Many measurements of the thermodynamic properties of C₃–to–C₈ hydrocarbons were carried out by Pitzer,^{1,2} Finke,^{3–6} Scott,⁷ Rossini,⁸ and Huffman^{9–12} prior to 1970. Building on these data, Benson^{13–16} developed empirical group additivity tables that became popular for estimating the thermodynamic properties of alkanes at various temperatures. A variety of statistical mechanical approximations^{17–20} have been used to estimate partition functions for *n*-butane, *n*-pentane, and other larger alkanes.²¹

The new results in the present paper are based on the nonempirical approach iii. We can distinguish two kinds of anharmonicity in alkane molecules that make it challenging to calculate the partition functions without using empirical data:^{22–24} (I) Multiple-structure anharmonicity is caused by the multiple minima of the potential energy surface that are encountered when one carries out internal rotation of the C–C bonds;

Department of Chemistry and Supercomputing Institute,
University of Minnesota, Minneapolis, Minnesota 55455-0431.
E-mail: truhlar@umn.edu

† Electronic supplementary information (ESI) available: Data used to calculate the partition functions using MS-AS-T and MS-AS-LH methods for *n*-heptane and isoheptane; coordinates of optimized structures of *n*-heptane and isoheptane. See DOI: 10.1039/c1cp22578b

in particular, the internal rotations generate many conformers of the alkane molecules, and the number becomes very large for longer alkanes. Even if high barriers separated these conformers, and even if the accessible configurations were locally harmonic, the existence of more than one minimum is a manifestation of the fact the potential energy surface is not globally quadratic, as required for the validity of the global harmonic approximation. (2) The torsional character of certain vibrations makes even the local application of the quadratic approximation quantitatively inaccurate, especially in the intermediate- and high-temperature range. Although hindered-rotor approximations^{17–20} using normal-mode-substitution models and mixed torsional Pitzer–Gwinn methods¹⁷ are available for statistical mechanical treatments of anharmonic molecules, it is still challenging to include multiple-structure anharmonicity and torsional anharmonicity when the torsions are not separable from each other and from other degrees of freedom. In addition, the internal rotation could couple with the overall rotation of the molecules; Wong and Raman addressed this issue in the study of the thermodynamic properties of 1,3-butadiene²⁵ and 1,2-dihaloethane²⁶ using an internal coordinate path Hamiltonian formalism.²⁷

Recently, we provided a new method, called the internal-coordinate multi-structural (MS) approximation²² to calculate the partition functions of complex molecules that contain several torsional modes and applied it to study the kinetics and thermodynamics of large molecules.^{23,24} This new method provides a practical approach to compute the partition functions of large molecules including both multiple-structure anharmonicity and torsional anharmonicity. The MS method with torsional anharmonicity (MS-T) includes both effects, and it reduces to the multi-structural local harmonic (MS-LH) approximation in the low-temperature limit, where only the multiple-structure anharmonicity effect is important; but it reaches the correct free-rotor result in the high-temperature limit, thereby including the torsional anharmonicity effect.

In the present work, we studied the thermal entropies, enthalpies, and free energies of the isomerization reaction between two alkanes: *n*-heptane and isoheptane. The *n*-heptane molecule contains six torsions, and four of them can generate distinguishable conformers; isoheptane also includes six torsions but only three of them produce distinguishable structures. Both multiple-structure and torsional anharmonicity play significant roles in both molecules and must be considered when calculating their partition functions and thermodynamic properties. In the present work we include all structures for each molecule, and we employ the MS method²² with both local harmonic and torsional anharmonicity approximations to calculate the conformational–vibrational–rotational partition functions, absolute entropies, and heat capacities of the two molecules and the changes of entropy, enthalpy, and free energy in the isomerization reaction that inter-converts the two molecules at various temperatures. We also utilized Benson’s empirical group additivity method to estimate the thermodynamic quantities of the two molecules. We will show that our calculated results agree well with experimental data from the American Petroleum Institute (API) tables,²⁸ with the Thermodynamics Research Center (TRC) data series,²⁹ and with the empirical estimates in the temperature range 298–1500 K, and extend our method to

calculate thermodynamic properties at even higher temperatures. Note that temperature of 3000 K and higher are not of practical interest for most purposes but are interesting to illustrate the approach to the high-temperature limiting form and therefore are included in two of the tables.

We note that the present work includes anharmonicity in three ways. First of all, calculated harmonic frequencies are scaled by an empirical factor of 0.981 that has been determined³⁰ to reduce the average error in zero point energies calculated by the local harmonic approximation. This factor includes all kinds of anharmonicity, both principal (*i.e.*, intra-mode) anharmonicity and mode-mode coupling.³¹ To be precise, then, because our zero point energies are based on these effective frequencies, our low temperature results should be called quasiharmonic, although we often omit the “quasi” since the method is general enough to include either true harmonic frequencies or effective frequencies. The second way in which we include anharmonicity is the multiple-structure effect. The existence of multiple local minima on a potential energy surface is an anharmonic effect since a harmonic oscillator has only one local minimum in its potential energy surface. Including all minima but treating each local minimum by the harmonic or quasiharmonic approximation is called the MS-LH approximation. (Notice, though, a possible semantic ambiguity since, from another point of view, the existence of multiple structures often (although not always) results from torsions, so the MS-LH treatment is the first step in taking account of torsions.) Finally we include explicit torsional anharmonicity, resulting in the MS-T approximation, which is designed to go to the correct high-temperature limit as far as torsions and overall rotations are concerned. But we should emphasize that we do not include other kinds of anharmonicity that become significant at high temperature. For example, principal bend anharmonicity^{32,33} could increase the partition function at high temperature (thereby partly cancelling the effect of torsional anharmonicity), but this is beyond the scope of the present treatment.

Finally we note that all calculations in the present paper refer to the vapor phase, and in particular for temperatures below the boiling point they refer to the saturated vapor phase in the standard state of an ideal gas at a partial pressure of one bar. To consider thermodynamics in the condensed phase would require considerations of intermolecular forces and packing. That is beyond our scope. In addition, note that some of our temperatures are above the auto-ignition temperatures of *n*-heptane and isoheptane, but this is not a concern because we study the pure hydrocarbon systems without any air or oxygen.

Computational methods

Electronic structure calculations

The M06-2X density functional³⁴ with the 6-311+G(2df,2p) basis set³⁵ was applied to optimize the geometries and obtain the frequencies for all the conformers of *n*-heptane and isoheptane. The 6-311+G(2df,2p) basis set is the same as the MG3S basis set³⁶ for H and C, and we will use the short name for brevity. The multilevel BMC-CCSD³⁷ method and the *ab initio* CCSD(T)-F12a^{38,39} method with the jul-cc-pVTZ basis set⁴⁰

were used to calculate single-point energies at the M06-2X optimized geometries.

M06-2X density functional calculations were performed by using the *Gaussian 09* program;⁴¹ the BMC-CCSD calculations were carried out using *MLGAUSS2.0*;⁴² and CCSD(T)-F12a calculations were performed using *Molpro*.⁴³ The integration grid employed for density functional calculations of frequencies had 99 radial shells and 974 angular points per shell.

The frequencies used for the partition function calculations in the next section are obtained by using M06-2X/MG3S density functional calculations and multiplying the directly calculated values by a quasiharmonic frequency scaling factor³⁰ specific for hydrocarbons; this factor is 0.981. This frequency factor is calibrated³⁰ to—on average—correct the zero point energy calculated from the frequencies by the harmonic formula; since the zero point energy is dominated by high-frequency modes, this factor applies mainly to high-frequency modes, and it may be considered to be part of the electronic structure methodology. In practice the factor is applied by multiplying all Cartesian and internal-coordinate Hessian elements by square of 0.981.³⁰

Conformational–vibrational–rotational partition functions

Including multiple structures and making the harmonic approximation in the vicinity of each local minimum of the potential energy surface is called the local harmonic (LH) approximation, and calculations including torsional anharmonicity have a suffix –T. If one uses all structures (AS), one may call the resulting multi-structural methods MS-AS-T and MS-AS-LH. However, in the rest of this paper (and in future work, except when we need to emphasize that all structures are included), we will shorten MS-AS-T and MS-AS-LH to MS-T and MS-LH, respectively; this will not cause confusion in the present paper because we always employ all structures in the present article. (MS-AS-T and MS-AS-LH were called MS-AS and MS-HO, respectively, in the original²² reference, but we now abandon that notation as being too easily misunderstood.)

The complete conformational–vibrational–rotational partition functions of *n*-heptane and isoheptane were calculated by the MS method²² using the *MSTor* program;⁴⁴ in the MS-LH and MS-T versions of this method we respectively have

$$Q_{\text{con-rovib}}^{\text{MS-LH}} = \sum_{j=1}^J Q_{\text{rot},j} \exp(-\beta U_j) Q_j^{\text{HO}} \quad (1)$$

and

$$Q_{\text{con-rovib}}^{\text{MS-T}} = \sum_{j=1}^J Q_{\text{rot},j} \exp(-\beta U_j) Q_j^{\text{HO}} Z_j \prod_{\tau=1}^t f_{j,\tau} \quad (2)$$

where “con” denotes conformational, “rovib” denotes rotational–vibrational; $Q_{\text{rot},j}$ is the rotational partition function (including the rotational symmetry number in the denominator) of structure j , Q_j^{HO} is the normal-mode local-harmonic-oscillator vibrational partition function calculated at structure j , Z_j is a factor designed to ensure that the MS-T scheme reaches the correct high- T limit (within the parameters of the model), and $f_{j,\tau}$ is an internal-coordinate torsional anharmonicity function that, in conjunction with Z_j , adjusts the harmonic partition function of structure j for the presence of the torsional motion τ .

Note that it is not necessary to assign each torsional motion to a specific normal mode. The MS-T approximation reduces to the MS-LH approximation in the low-temperature limit, and it approaches the free-rotor result in the high-temperature limit. The Z_j and $f_{j,\tau}$ factors, based in part on internal-coordinate Hessians, are designed to interpolate the partition function between these limits in the intermediate temperature range. In principle, more accurate interpolations could be carried out²² if one calculated the barrier heights for torsional motions that interconvert the reactant structures with one another and the transition state structures with one another, but an advantage of the method employed here is that it does not require the expensive and labor-intensive step of finding and characterizing saddle points.

Thermodynamic function calculations

The energy and entropy functions can be calculated using the complete partition functions (including translational, electronic, and conformational–vibrational–rotational contributions) by the following:

$$E = - \frac{\partial \ln(Q)}{\partial \beta} \quad (3)$$

$$S^\circ = k_B + k_B \ln Q - \frac{1}{T} \left(\frac{\partial \ln Q}{\partial \beta} \right)_V \quad (4)$$

where $Q = Q_{\text{el}} Q_{\text{t}} Q_{\text{con-rovib}}$ in which Q_{el} and Q_{t} are electronic and translational partition functions, respectively. The translational partition function is evaluated for one mole of an ideal gas at a standard state pressure of one bar (0.986923 standard atmospheres).

Then the enthalpy and free energy can be obtained by

$$H = E + k_B T \quad (5)$$

$$G^\circ = H - TS^\circ \quad (6)$$

The heat capacity C_p can be determined using

$$C_p = \left(\frac{\partial H}{\partial T} \right)_p \quad (7)$$

Results and discussion

Structures, energies, and rotational symmetry number of *n*-heptane

We label the carbons of *n*-heptane as shown in Fig. 1. There are six internal rotation coordinates in the molecule, which describe torsions around the C(1)–C(2), C(2)–C(3), C(3)–C(4), C(4)–C(5), C(5)–C(6), and C(6)–C(7) bonds. Note that the torsional motions of the methyl groups, –C(1)H₃ and –C(7)H₃, in the molecule do not generate distinct structures due to the symmetry. Therefore, only the C(2)–C(3), C(3)–C(4), C(4)–C(5), and C(5)–C(6) torsional motions produce distinguishable conformers. Based on calculations using the M06-2X density functional with the MG3S basis set, 59 distinguishable structures (conformers) of *n*-heptane have been obtained in the present work, and 58 of them consist of 29 pairs of mirror images. The remaining structure, due to symmetry (it has a mirror plane) does not have a distinguishable mirror image.

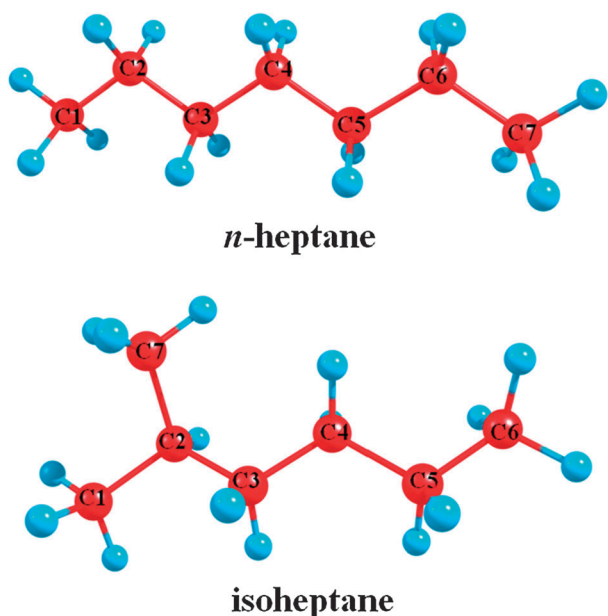


Fig. 1 Numbering scheme for *n*-heptane and isoheptane.

Fig. 2 shows 30 structures of *n*-heptane. Except for the first structure, all the others have corresponding mirror-image structures. Tables 1 and 2 show the naming convention and structural numbering that is used for labeling the structures. For instance, “**ap⁺sc⁺ac⁺ap⁺**” (structure 26) means the conformer of *n*-heptane with the first, second, third, and fourth dihedral angles in the ranges of 150 to 180, 30 to 60 and 90 to 120, and 150 to 180 degrees, respectively. Note that the structure **apapapap** has no mirror image pair due to its C_{2v} symmetry. The relative conformational energetic information and rotational symmetry numbers of these 59 structures are specified in Table 2. It is found that the BMC-CCSD and M06-2X

energies agree very well with each other, but, for each of the structures, they are consistently smaller than the energies calculated by CCSD(T)-F12a. The deviations between the M06-2X energy and the CCSD(T)-F12a energy range from 0.19 to 1.39 kcal/mol. Note that there are 11 structures (including the global minimum structure, and the highest-energy local-minimum structure), that contain a C_2 rotational axis, and the corresponding rotational symmetry number of these structures is 2. This symmetry number reduces the contributions of these structures to the conformational–vibrational–rotational partition functions.

Structures, energies, and rotational symmetry number of isoheptane

Isoheptane also contains six internal rotations, and the labeling of the carbon backbone is also displayed in Fig. 1. The torsional motions are around the C(1)–C(2), C(2)–C(3), C(3)–C(4), C(4)–C(5), C(5)–C(6), and C(2)–C(7) bonds. The internal rotation of the three methyl groups –C(1)H₃, –C(6)H₃, and –C(7)H₃ generates identical conformers; thus they do not contribute to the multiple-structure effect, whereas the torsional motions around the C(2)–C(3) and C(3)–C(4), and C(4)–C(5) bonds do produce distinguishable conformers. In total, 37 structures were obtained for isoheptane using the M06-2X density functional in the present work, and they are shown in Fig. 3. Tables 1 and 3 show the naming and numbering convention that is used for labeling of the structures, and the relative conformational energy and rotational symmetry number of each structure are given in the Table 3. As for *n*-heptane, the relative conformational energies calculated using CCSD(T)-F12a are larger than those calculated with either BMC-CCSD or M06-2X. The deviations between the M06-2X and CCSD(T)-F12a results are smaller than those for *n*-heptane; they range from 0.12 to 1.09 kcal/mol. None of the

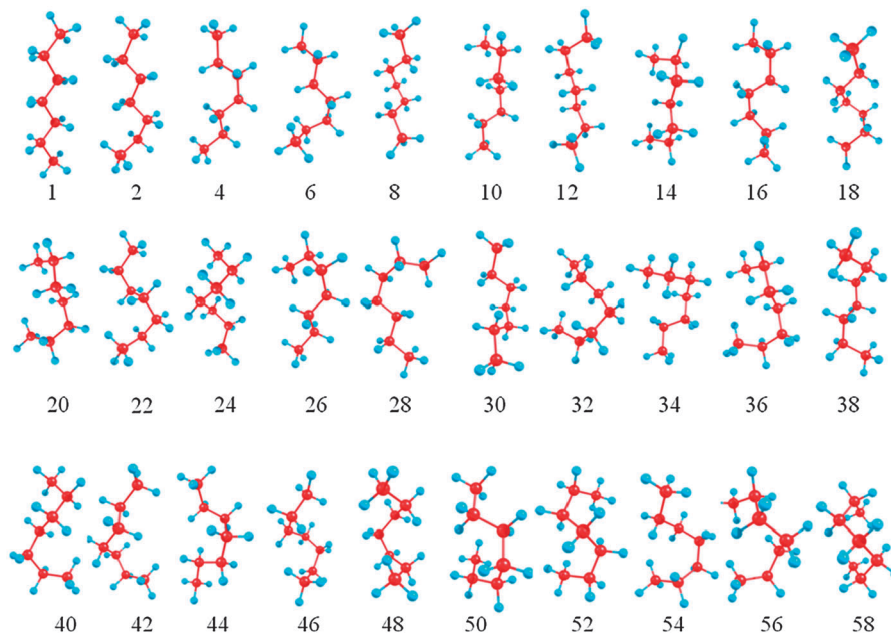


Fig. 2 Structures of *n*-heptane. Note that all structures shown except structure 1 also have distinguishable mirror images. This figure is also included in ESI as Fig. S1.†

Table 1 Labeling of structures^a

	Abbreviation	dihedral angle range (deg)
+ syn-periplanar	sp +	[0, 30]
− syn-periplanar	sp −	[−30, 0]
+ syn-clinal	sc +	[30, 60]
− syn-clinal	sc −	[−60, −30]
+ gauche	g +	[60, 90]
− gauche	g −	[−90, −60]
+ anti-clinal	ac +	[90, 120]
− anti-clinal	ac −	[−120, −90]
+ anti-periplanar	ap +	[150, 180]
− anti-periplanar	ap −	[−180, −150]
anti-periplanar	ap	180

^a The dihedral angles in used for torsions are and C(1)–C(2)–C(3)–C(4), C(2)–C(3)–C(4)–C(5), C(3)–C(4)–C(5)–C(6), and C(4)–C(5)–C(6)–C(7) for *n*-heptane; the dihedral angles in used for torsions are and C(1)–C(2)–C(3)–C(4), C(2)–C(3)–C(4)–C(5), and C(3)–C(4)–C(5)–C(6) for isoheptane.

structures has a rotational symmetry axis; thus the overall rotational symmetry numbers of all structures are one.

Conformational–vibrational–rotational partition functions of *n*-heptane and isoheptane in various approximations

The number of structures of each isomer provides the first indication that the torsions are strongly coupled. For *n*-heptane, excluding the two methyl torsions, because methyl torsions do not generate more than one distinguishable structure, gives four torsions, and four independent torsions generate n^4 structures where n is the number of structures generated by an independent torsion. For ideal torsions, n would be 3 (two gauche and one trans conformer) and n^4 would equal 81, but we find only 59 distinguishable structures. For isoheptane, separable ideal torsions would generate $3^3 = 27$ structures, but we instead find 37 distinguishable structures. To understand these differences we must consider two issues: rotational symmetry and the pentane effect.

First consider rotational symmetry. As explained in the original MS-T paper,²² the Voronoi calculation of the effective periodicities includes not just the indistinguishable structures, but also all the distinguishable structures located in the full torsion space. For example, in *n*-heptane, starting from the all-trans structure (structure 1), rotation of the C(2)–C(3), C(3)–C(4), C(4)–C(5) and C(5)–C(6) bonds by −122.95, −122.26, −116.63, and −270.06 degrees, respectively, gives the same structure (structure $sc^+sc^+g^+ac^-$) as is obtained by rotation of these bonds by −270.06, −116.63, −122.26, and −122.95 degrees, respectively. Although there is only one distinguishable structure generated, both of these structures must be included in the torsional space for the effective periodicity calculations. For the present molecules, this kind of phenomenon occurs in *n*-heptane but not in isoheptane. In fact, counting both distinguishable structures and indistinguishable ones, *n*-heptane has 107 structures; these consist of 11 structures with a rotational symmetry number of two and 96 structures with a rotational symmetry of one, but overall rotations map 48 of these into the other 48, so the final number of distinguishable structures is 59. Thus, in considering the torsional landscape one must actually compare 107 structures (not 59) to the ideal number of 81 for *n*-heptane. For isoheptane, there is no rotational symmetry,

Table 2 Name convention, sequence number, energy^a (kcal/mol), and rotational symmetry number of *n*-heptane^a

Structures	Number <i>j</i>	Energy			σ_j
		M06-2X	BMC-CCSD	CCSD(T)-F12a	
apapapap	1	0.00	0.00	0.00	2
ap ap g ap [−] , ap ⁺ ap ⁺ g ⁺ ap [−]	2, 3	0.47	0.46	0.58	1
ap ap sc sc [−] , ap ⁺ ap ⁺ sc ⁺ sc ⁺	4, 5	0.47	0.41	0.57	1
ap ap ap g [−] , ap ⁺ ap ⁺ ap ⁺ g ⁺	6, 7	0.47	0.48	0.86	1
ap ⁺ sc ⁺ sc ⁺ ap ⁺ , ap [−] sc [−] sc [−] ap [−]	8, 9	0.48	0.43	0.85	2
ap ⁺ sc ⁺ sc ⁺ sc ⁺ , ap [−] sc [−] sc [−] sc [−]	10, 11	0.88	0.86	1.13	1
sc ⁺ sc ⁺ sc ⁺ sc ⁺ , sc [−] sc [−] sc [−] sc [−]	12, 13	0.92	0.88	1.14	2
sc [−] sc [−] sc [−] sc [−] , g ⁺ ap ⁺ sc ⁺ sc ⁺	14, 15	0.98	0.91	1.15	1
g [−] ap [−] sc [−] sc [−] , ap ⁺ g ⁺ ap ⁺ g ⁺	16, 17	1.11	1.03	1.25	1
ap [−] g [−] ap [−] g [−] , g ⁺ ap ⁺ ap ⁺ g ⁺	18, 19	0.49	0.54	1.13	1
g [−] ap [−] ap [−] g [−] , g ⁺ ap ⁺ ap ⁺ g ⁺	20, 21	0.82	0.86	1.37	1
g [−] ap [−] ap [−] g [−] , g ⁺ ap ⁺ sc ⁺ sc ⁺	22, 23	1.09	1.09	1.56	1
g [−] ap [−] sc ⁺ sc ⁺ , ap ⁺ g ⁺ ap ⁺ g ⁺	24, 25	0.54	0.71	1.46	2
ap [−] g [−] ap [−] g [−] , ap ⁺ sc ⁺ ac ⁺ ap ⁺	26, 27	2.25	2.31	2.58	1
ap [−] sc [−] ac [−] ap [−] , ap ⁺ g ⁺ sc ⁺ ac ⁺	28, 29	2.35	2.35	2.66	1
ap [−] g [−] sc [−] ac [−] , ap ⁺ ap ⁺ ac ⁺ sc ⁺	30, 31	2.18	2.18	2.50	1
ap [−] ap [−] ac [−] sc [−] , ap ⁺ ap ⁺ g ⁺ g ⁺	32, 33	2.25	2.3	2.88	1
ap [−] ap [−] g [−] g [−] , ap ⁺ ap ⁺ sc ⁺ ac ⁺	34, 35	2.29	2.31	2.83	1
ap ⁺ ap ⁺ sc ⁺ ac ⁺ , sc ⁺ sc ⁺ g ⁺ ac ⁺	36, 37	2.68	2.74	3.14	1
sc [−] sc [−] g [−] ac [−] , g ⁺ g ⁺ ac ⁺ g ⁺	38, 39	2.81	2.86	3.25	1
g [−] g [−] ac [−] g [−] , g ⁺ ap ⁺ ac ⁺ sc ⁺	40, 41	2.72	2.86	3.24	1
g [−] ap [−] ac [−] sc [−] , g ⁺ ap ⁺ ac ⁺ sc ⁺	42, 43	2.81	2.81	3.17	1
g [−] ap [−] ac [−] sc [−] , ap ⁺ sc ⁺ ac ⁺ g ⁺	44, 45	2.77	2.73	3.13	1
ap [−] sc [−] ac [−] g [−] , ap ⁺ g ⁺ ac ⁺ sc ⁺	46, 47	2.59	2.72	3.39	1
ap ⁺ g ⁺ ac ⁺ sc ⁺ , sc [−] ap [−] g [−] g [−]	48, 49	2.67	2.69	3.37	1
sc [−] ap [−] g [−] g [−] , ap ⁺ ac ⁺ g ⁺ g ⁺	50, 51	3.88	3.94	4.72	1
ap ⁺ ac ⁺ g ⁺ g ⁺ , sc ⁺ ac ⁺ ac ⁺ sc ⁺	52, 53	3.92	4.19	4.85	2
sc [−] ac [−] ac [−] sc [−] , g ⁺ ac ⁺ g ⁺ ac ⁺	54, 55	4.75	4.72	5.36	1
g [−] ac [−] g [−] ac [−] , ac ⁺ g ⁺ ac ⁺ sc ⁺	56, 57	5.29	5.39	5.88	1
ac [−] g [−] ac [−] sc [−] , ac ⁺ g ⁺ g ⁺ ac ⁺	58, 59	5.61	5.67	6.18	2
ac [−] g [−] g [−] ac [−]					

^a The energy is calculated by the M06-2X, BMC-CCSD, and CCSD(T)-F12a methods, respectively. If overall rotation maps a structure onto the same unique nonisomorphic conformer, then the rotated image is not counted, and a rotational symmetry number of two is included in the rotational partition function of the original structure. If overall rotation maps a structure onto a different structure from the list constructed considering only torsional symmetry, then we include only one of them and use a rotational symmetry number of one.

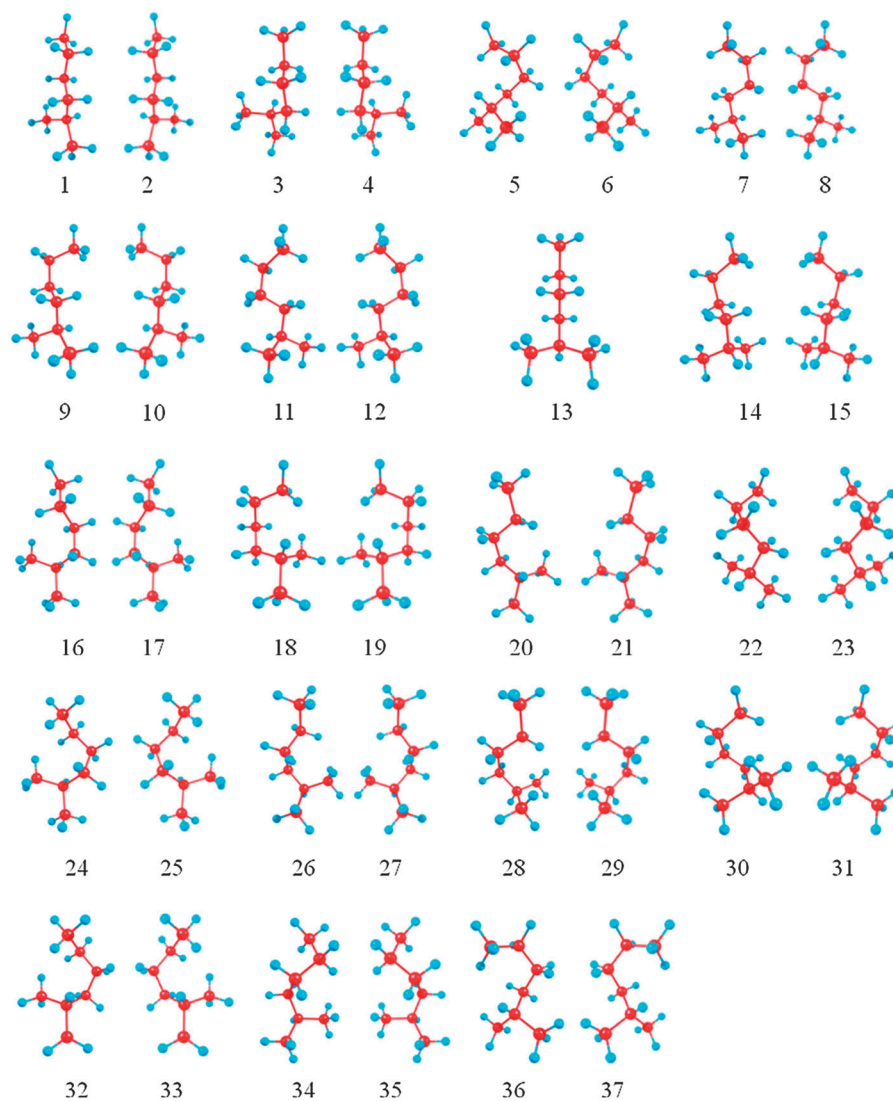


Fig. 3 Structures of isoheptane. All structures occur in optically active pairs except structure 13. This figure is also included in ESI as Fig. S2.†

so one must compare 37 structures to the ideal number of 27 in this case.

Next consider the pentane effect. For alkane or polyethylene chains of length five carbons or longer, it is well known that structures with $\mathbf{g}^+\mathbf{g}^-$ or $\mathbf{g}^-\mathbf{g}^+$ configurations for successive torsions are either excluded or made unfavorable by steric repulsion; this is called the pentane effect.^{45–63} Naively one might simply assume that these structures are missing and that the number of structures would be less than the ideal number. In fact, Tables 2 and 3 show that none of the *n*-heptane or isoheptane structures contains $\mathbf{g}^+\mathbf{g}^-$ or $\mathbf{g}^-\mathbf{g}^+$. However, the situation is actually more complicated because the pentane effect can also make the conformational landscape more rugged. The sterically disfavored structure may, for example, be replaced by two structures,^{21,47,54,55,57} for instance, in isoheptane the $\mathbf{g}^+\mathbf{g}^-$ conformation of C(1)–C(2)–C(3)–C(4), C(2)–C(3)–C(4)–C(5) is replaced by two structures: with $\mathbf{g}^+\mathbf{sc}^-$ for these torsions in structure 3 and with $\mathbf{sc}^+\mathbf{g}^-$ for these torsions in structure 18. This kind of effect makes the total number of conformers larger than the ideal number, and this added ruggedness explains why

both *n*-heptane and isoheptane have more structures than the ideal number (107 vs. 81 and 37 vs. 27).

If one creates a list of 27 ideal structures for isoheptane by simply assigned \mathbf{ap} , \mathbf{g}^+ , or \mathbf{g}^- to every torsion in all combinations, one finds that 15 of the 27 ideal structures have neither $\mathbf{g}^+\mathbf{g}^-$ nor $\mathbf{g}^-\mathbf{g}^+$, and 10 have one of these, and two have two of them. Replacing each of the 12 disfavored structures by 2 structures yields the total of 37 structures that are observed.

The existence of this kind of ruggedness provides further confirmation that the torsional motion must be considered strongly coupled in partition function calculations.

We can compare some details of our structure counts for *n*-heptane to previous work. For this purpose we introduce the term “unique (nonisomorphic) conformers” used by Tasi *et al.*⁵⁷ to denote the number of structures excluding those generated from ones already in the list by 180 deg rotation (here we are referring to overall rotation) or mirror reflection; Goto *et al.*⁵⁵ call these generatable conformers “symmetrically equivalent conformers”. Scott and Scheraga⁴⁵ used a molecular mechanics potential functions and found 28 unique nonisomorphic

Table 3 Name convention, sequence number, energy^a (kcal/mol), and rotational symmetry number of isoheptane

Structures	Number <i>j</i>	Energy			σ_j
		M06-2X	BMC-CCSD	CCSD(T)-F12a	
sc ⁻ ap ⁻ ap ⁻ , sc ⁺ ap ⁺ ap ⁺	1, 2	0.00	0.00	0.00	1
g ⁺ sc ⁻ ap ⁻ , g ⁻ sc ⁺ ap ⁺	3, 4	0.01	0.03	0.30	1
g ⁺ sc ⁻ sc ⁻ , g ⁻ sc ⁺ sc ⁺	5, 6	0.02	0.09	0.57	1
sc ⁻ ap ⁺ g ⁺ , sc ⁺ ap ⁻ g ⁻	7, 8	0.37	0.4	0.53	1
sc ⁺ ap ⁺ g ⁺ , sc ⁻ ap ⁻ g ⁻	9, 10	0.65	0.59	0.69	1
g ⁺ ap ⁻ sc ⁻ , g ⁻ ap ⁺ sc ⁺	11, 12	0.68	0.70	0.90	1
apapap	13	0.69	0.67	0.75	1
ap ⁺ ap ⁺ g ⁺ , ap ⁻ ap ⁻ g ⁻	14, 15	1.22	1.24	1.43	1
g ⁺ ac ⁺ ap ⁺ , g ⁻ ac ⁻ ap ⁻	16, 17	1.70	1.81	1.95	1
sc ⁺ g ⁻ ac ⁺ , sc ⁻ g ⁺ ac ⁻	18, 19	1.98	2.04	2.43	1
sp ⁺ sc ⁺ ap ⁺ , sp ⁻ sc ⁻ ap ⁻	20, 21	2.18	2.17	2.36	1
g ⁻ ac ⁻ g ⁻ , g ⁺ ac ⁺ g ⁺	22, 23	2.26	2.32	2.54	1
sp ⁺ g ⁺ g ⁺ , sp ⁻ g ⁻ g ⁻	24, 25	2.29	2.32	2.70	1
ap ⁻ ac ⁺ ap ⁻ , ap ⁺ ac ⁻ ap ⁺	26, 27	2.42	2.48	2.69	1
ap ⁺ g ⁺ ap ⁺ , ap ⁻ g ⁻ ap ⁻	28, 29	2.60	2.67	2.98	1
ap ⁺ g ⁺ sc ⁺ , ap ⁻ g ⁻ sc ⁻	30, 31	2.61	2.83	3.34	1
sc ⁻ g ⁻ ac ⁺ , sc ⁺ g ⁺ ac ⁻	32, 33	4.09	4.08	4.50	1
ap ⁻ ac ⁺ g ⁺ , ap ⁺ ac ⁻ g ⁻	34, 35	3.06	3.10	3.38	1
sc ⁺ ac ⁺ g ⁺ , sc ⁻ ac ⁻ g ⁻	36, 37	2.16	2.18	2.48	1

^a The energy is calculated by the M06-2X, BMC-CCSD, and CCSD(T)-F12a methods, respectively. If overall rotation maps a structure onto the same unique nonisomorphic conformer, then the rotated image is not counted, and a rotational symmetry number of two is included in the rotational partition function of the original structure. If overall rotation maps a structure onto a different structure from the list constructed considering only torsional symmetry, then we include only one of them and use a rotational symmetry number of one.

conformers and a total of 101 conformers in the full torsional space; Goto *et al.* used the MM2 molecular mechanics method to explore the torsional landscape and they found 31 unique nonisomorphic conformers and a total of 109 conformers in the full torsional space; Tasi *et al.* used a parametrized effective one-electron quantum chemical model and found 30 unique nonisomorphic conformers and a total of 107 conformers in the full torsional space; and we find 30 unique nonisomorphic conformers (the 30 rows of Table 2) and a total of 107 conformers in the full torsional space. The agreement of these numbers of structures is

reasonable since different electronic structure or molecular mechanics methods do not necessarily predict the same number of structures and furthermore the higher-energy ones might easily be missed in searches.

It is worthwhile to emphasize some statistical mechanical issues here. Goto⁵⁵ assigned each of the conformers a “statistical weight” equal to one plus the number of structures generated from it by 180 deg rotation, mirror reflection, or a combination of rotation and reflection. That is correct for the structures generated by mirror reflection but not for the structures generated from the original structure or its mirror image by rotation. If overall rotation maps a structure onto the same unique nonisomorphic conformer, then the rotated image should not be counted, and furthermore a rotational symmetry number of two should be included in the rotational partition function of the original structure. If overall rotation maps a structure into a different structure from the list constructed considering only torsional symmetry, then one has two choices: either (i) count both and use a rotational symmetry number of 2 for both or (ii) count only one of them and use a rotational symmetry number of one. We make the latter choice (although the first choice might be preferred by some because it has the advantage that the rotational symmetry number is the same for every structure). Scott and Scheraga⁴⁵ computed a “statistical weight” in the same way as Goto *et al.*, but they did not perform statistical mechanical calculations. Tasi *et al.*⁵⁷ include self-images that are equivalent by rotation in their figures.

The partition functions calculated for *n*-heptane and isoheptane in the present work are given in Tables 4 and 5. The zero of energy for the partition function calculations is taken to be the energy at the global minimum structure of the isomer under consideration, *n*-heptane or isoheptane. In *n*-heptane, four of the torsions [C(2)–C(3), C(3)–C(4), C(4)–C(5) and C(5)–C(6)] are involved in a strongly coupled²² (SC) group; the other two torsions [C(1)–C(2), C(6)–C(7)] are considered to be nearly separable (NS). In isoheptane, three torsions [C(2)–C(3) and C(3)–C(4), and C(4)–C(5)] are strongly coupled and the other three [C(1)–C(2) and C(5)–C(6), and C(2)–C(7)] are treated as nearly separable torsions. The nearly separable torsions are all internal rotations of methyl groups that produce

Table 4 Calculated conformational-vibrational-rotational partition function of *n*-heptane

<i>T</i> (K)	MS-LH			MS-T		
	M06-2X	BMC-CCSD ^a	CCSD(T)-F12a ^b	M06-2X	BMC-CCSD ^a	CCSD(T)-F12a ^b
298	2.85E – 90	2.63E – 90	1.89E – 90	4.20E – 90	3.88E – 90	2.80E – 90
300	1.39E – 89	1.28E – 89	9.20E – 90	2.05E – 89	1.89E – 89	1.37E – 89
400	1.09E – 63	1.02E – 63	7.73E – 64	1.88E – 63	1.76E – 63	1.35E – 63
500	1.13E – 47	1.07E – 47	8.44E – 48	2.23E – 47	2.11E – 47	1.68E – 47
600	1.34E – 36	1.27E – 36	1.04E – 36	2.92E – 36	2.78E – 36	2.81E – 36
800	6.68E – 22	6.42E – 22	5.45E – 22	1.63E – 21	1.57E – 21	1.34E – 21
1000	3.13E – 12	3.03E – 12	2.64E – 12	7.84E – 12	7.59E – 12	6.65E – 12
1500	3.56E + 03	3.48E + 03	3.16E + 03	7.93E + 03	7.75E + 03	7.04E + 03
2000	1.02E + 13	1.00E + 13	9.32E + 12	1.82E + 13	1.79E + 13	1.66E + 13
2400	4.86E + 18	4.79E + 18	4.50E + 18	7.14E + 18	7.04E + 18	6.59E + 18
3000	2.61E + 25	2.58E + 25	2.45E + 25	2.85E + 25	2.82E + 25	2.67E + 25
4000	7.20E + 33	7.14E + 33	6.87E + 33	4.98E + 33	4.94E + 33	4.73E + 33
6000	3.16E + 45	3.14E + 45	3.06E + 45	9.98E + 44	9.94E + 44	9.63E + 44
8000	4.59E + 53	4.57E + 53	4.48E + 53	7.70E + 52	7.67E + 52	7.49E + 52
10000	9.18E + 59	9.15E + 59	9.00E + 59	9.06E + 58	9.03E + 58	8.85E + 58

^a BMC-CCSD//M06-2X/MG3S. ^b CCSD(T)-F12a/jul-cc-pVTZ//M06-2X/MG3S.

Table 5 Calculated conformational-vibrational-rotational partition function of isoheptane

T (K)	MS-LH			MS-T		
	M06-2X	BMC-CCSD ^a	CCSD(T)-F12a ^b	M06-2X	BMC-CCSD ^a	CCSD(T)-F12a ^b
298	3.03E - 90	3.04E - 90	2.55E - 90	4.45E - 90	4.46E - 90	3.76E - 90
300	1.47E - 89	1.47E - 89	1.23E - 90	2.16E - 89	2.17E - 89	1.83E - 89
400	9.35E - 64	9.36E - 64	8.09E - 64	1.61E - 63	1.61E - 63	1.40E - 63
500	8.71E - 48	8.71E - 48	7.68E - 48	1.70E - 47	1.70E - 47	1.51E - 47
600	9.67E - 37	9.66E - 37	8.66E - 36	2.07E - 36	2.08E - 36	1.87E - 36
800	4.49E - 22	4.48E - 22	4.10E - 22	1.07E - 21	1.07E - 21	9.82E - 22
1000	2.02E - 12	2.02E - 12	1.88E - 12	4.92E - 12	4.92E - 12	4.58E - 12
1500	2.20E + 03	2.19E + 03	2.08E + 03	4.71E + 03	4.70E + 03	4.46E + 03
2000	6.17E + 12	6.15E + 12	5.91E + 12	1.06E + 13	1.05E + 13	1.01E + 13
2400	2.90E + 18	2.90E + 18	2.80E + 18	4.07E + 18	4.06E + 18	3.91E + 18
3000	1.54E + 25	1.54E + 25	1.49E + 25	1.61E + 25	1.60E + 25	1.55E + 25
4000	4.20E + 33	4.20E + 33	4.10E + 33	2.77E + 33	2.76E + 33	2.69E + 33
6000	1.82E + 45	1.82E + 45	1.79E + 45	5.50E + 44	5.48E + 44	5.38E + 44
8000	2.63E + 53	2.63E + 53	2.60E + 53	4.23E + 52	4.22E + 52	4.16E + 52
10000	5.24E + 59	5.23E + 59	5.19E + 59	4.97E + 58	4.96E + 58	4.90E + 58

^a BMC-CCSD//M06-2X/MG3S. ^b CCSD(T)-F12a/jul-cc-pVTZ//M06-2X/MG3S.

three identical structures. For these torsions we can take $M_{j,\tau}$ (the total number of minima, whether distinguishable or not, along torsional coordinate τ of structure j) as three. For the strongly coupled torsions, the $M_{j,\tau}$ parameters are obtained by four-dimensional and three-dimensional Voronoi tessellation methods^{22,44} for n -heptane and isoheptane, respectively. Tables S1 and S2 in the ESI† give full details of the torsional parameters for each structure of n -heptane and isoheptane that are used for the partition function calculations carried out using MS-T approximation by the *MSTor* program.⁴⁴

Tables 4 and 5 show that the partition functions obtained by CCSD(T)-F12a are smaller than those by BMC-CCSD, which are smaller than those by M06-2X. The percent deviations between CCSD(T)-F12a and M06-2X results decrease with temperature for both n -heptane and isoheptane as shown in Fig. 4 and 5. The percent deviations between BMC-CCSD and M06-2X decrease with increase of temperature for n -heptane, but they are close to zero for isoheptane as shown in Fig. 4 and 5. These temperature-dependent behaviors of deviations are understandable since the differences of the conformation energies calculated by CCSD(T)-F12a and M06-2X are large, but those between BMC-CCSD and M06-2X are small.

For n -heptane, Table 4 and Fig. 6 show the differences of the partition functions calculated by the MS-LH and MS-T approximations. Two asymptotic trends have been correctly designed into the approximations:²² (1) In the limit where the temperature approaches zero, the ratio $Q_{\text{con-rovib}}^{\text{MS-T}}/Q_{\text{con-rovib}}^{\text{MS-LH}}$ goes to one; and (2) as the temperature tends to infinity, the ratio goes to zero. As the temperature increases from zero, the $Q_{\text{con-rovib}}^{\text{MS-T}}/Q_{\text{con-rovib}}^{\text{MS-LH}}$ ratio first increases dramatically and then decreases gradually. At low temperature the LH approximation underestimates the partition functions, and at high T it overestimates it. Similar behavior is observed in Table 5 and Fig. 7 for isoheptane.

Interestingly, it is found that the ratio of isoheptane partition functions to n -heptane partition functions decays dramatically with increasing temperature and then reaches a steady value at the high-temperature limit in both MS-LH and MS-T calculations, as shown in Fig. 8. In the MS-T approximation, at 298 K the ratio is 1.34, 1.15, or 1.06 for CCSD(T)-F12a,

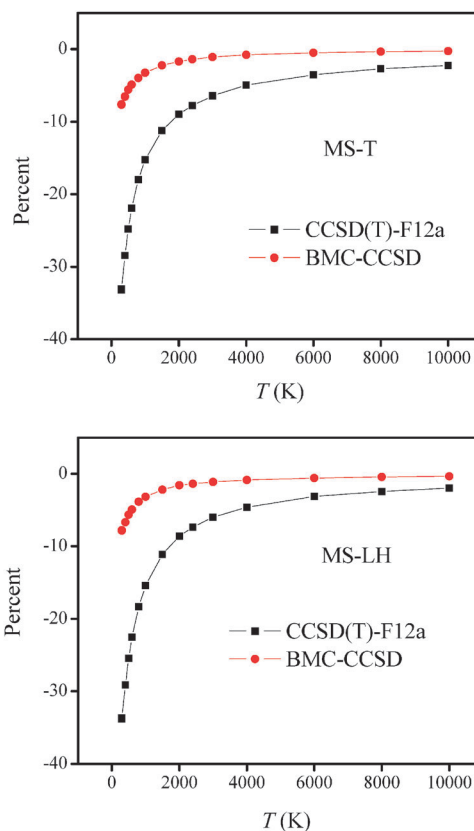


Fig. 4 The percent deviations of partition functions of n -heptane between CCSD(T)-F12a and M06-2X results, and the percent deviations between BMC-CCSD and M06-2X results calculated by MS-LH and MS-T methods.

BMC-CCSD, or M06-2X calculations, respectively; and at 10000 K, the ratio becomes 0.55, 0.55, and 0.55. As already noted, n -heptane has 59 structures and isoheptane has 37, and these two numbers are correlated with the asymptotic behavior in the high-temperature range. Based on CCSD(T)-F12a, BMC-CCSD, and M06-2X calculations, the relative conformational energies have a spread from 0 to 6.18, 5.67, and

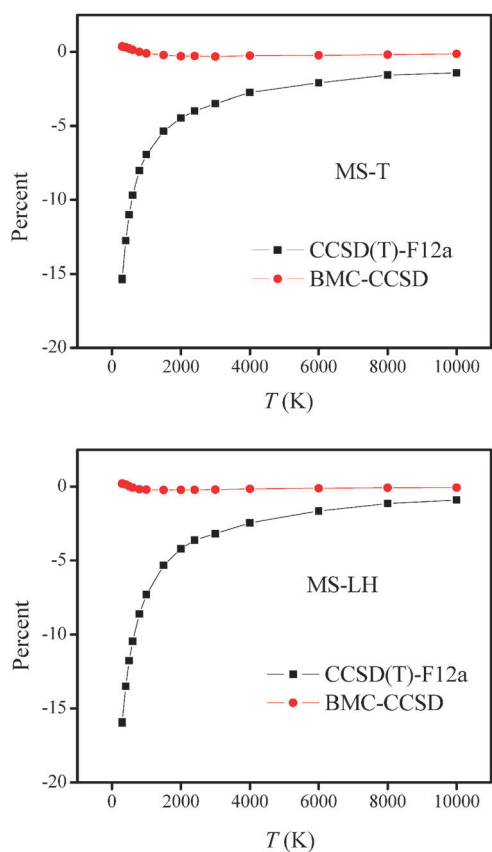


Fig. 5 The percent deviations of partition functions of isoheptane between CCSD(T)-F12a and M06-2X results, and the percent deviations between BMC-CCSD and M06-2X results calculated by MS-LH and MS-T methods.

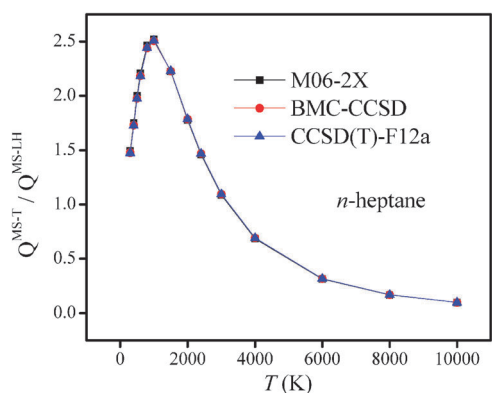


Fig. 6 The ratio of partition functions of *n*-heptane calculated by MS-T and MS-LH approximations at various temperatures.

5.61 kcal/mol for *n*-heptane, and range from 0 to 4.50, 4.08, and 4.09 kcal/mol for isoheptane. Because of the higher conformational energies of *n*-heptane, at low temperature many conformers contribute much less to the total partition functions than for isoheptane; thus its partition functions are smaller. When temperature increases, the contribution from higher-energy conformers becomes significant, and the partition functions of *n*-heptane become larger than those of isoheptane.

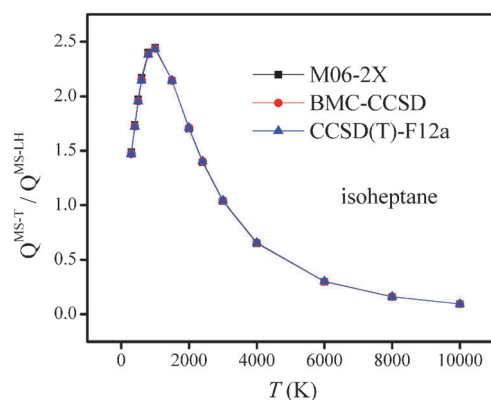


Fig. 7 The ratio of partition functions of isoheptane calculated by MS-T and MS-LH approximations at various temperatures.

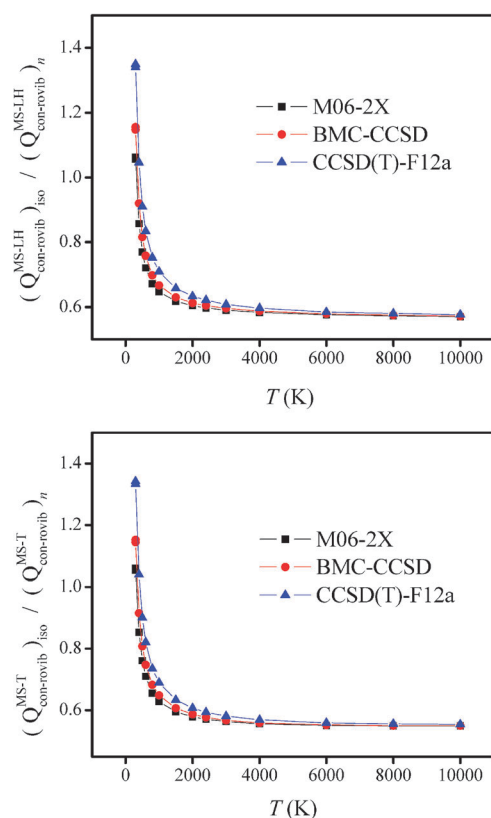


Fig. 8 The ratio of partition functions of isoheptane over *n*-heptane calculated by MS-LH and MS-T approximations at various temperatures.

Entropies and heat capacities of *n*-heptane and isoheptane

We employed the eqn (3), (4), (5), and (7) to calculate the standard-state entropy and heat capacity of *n*-heptane and isoheptane. The results are given in the Tables 6–9. In addition, we apply Benson's group additivity parameters^{13,15} to estimate the same thermodynamic quantities, and these results are also tabulated in Tables 6–9. Note that Benson's heat-of-formation parameters in ref. 15 are updated from those in ref. 13, but the entropy and heat capacity parameters are still the same as those in ref. 13. (Because Benson's parameters and the thermodynamic functions in the API tables correspond to

Table 6 Standard-state entropy of *n*-heptane in cal mol⁻¹ K⁻¹ at various temperatures

<i>T</i> (K)	MS-LH			MS-T			Benson ^c	Exp.-API ^d	Exp.-TRC ^e	Exp ^f
	M06-2X	BMC-CCSD ^a	CCSD(T)-F12a ^b	M06-2X	BMC-CCSD ^a	CCSD(T)-F12a ^b				
298	101.44	101.35	101.05	103.16	103.08	102.81	102.21	102.27	102.32	
300	101.69	101.60	101.31	103.43	103.35	103.08	102.48	102.53	102.56	
371.5	110.57	110.52	110.32	112.71	112.66	112.48	111.81			111.80 ± 0.3
400	114.06	114.02	113.84	116.32	116.28	116.12	115.44	115.45	115.44	
500	126.12	126.09	125.96	128.63	128.60	128.49	127.76	127.77	127.75	
600	137.77	137.75	137.65	140.33	140.30	140.21	139.45	139.42	139.53	
800	159.56	159.55	159.49	161.84	161.83	161.76	160.98	160.98	161.23	
1000	179.28	179.27	179.23	181.09	181.08	181.02	180.26	180.25	180.52	
1500	220.79	220.78	220.76	221.28	221.28	221.23	220.40		220.60	
2000	253.80	253.79	253.78	253.09	253.09	253.06				
2400	275.81	275.81	275.80	274.27	274.28	274.25				

^a BMC-CCSD//M06-2X/MG3S. ^b CCSD(T)-F12a/jul-cc-pVTZ//M06-2X/MG3S. ^c Using Benson's data from ref. 13 and adding 0.026 cal mol⁻¹ K⁻¹ to convert from a standard pressure of 1 atm to a standard pressure of 1 bar. ^d Using API data from ref. 28 and adding 0.026 cal mol⁻¹ K⁻¹ to convert from a standard pressure of 1 atm to a standard pressure of 1 bar. ^e Using TRC data from ref. 29. ^f The experimental data come from ref. 63, and we added 0.026 cal mol⁻¹ K⁻¹ to convert from a standard pressure of 1 atm to a standard pressure of 1 bar.

Table 7 Standard-state entropy of isoheptane in cal mol⁻¹ K⁻¹ at various temperatures

<i>T</i> (K)	MS-LH			MS-T			Benson ^c	Exp.-API ^d	Exp.-TRC ^e
	M06-2X	BMC-CCSD ^a	CCSD(T)-F12a ^b	M06-2X	BMC-CCSD ^a	CCSD(T)-F12a ^b			
298	99.76	99.77	99.62	101.48	101.49	101.36	100.90	100.38	100.50
300	100.02	100.02	99.88	101.75	101.76	101.63	101.16	100.62	100.74
400	112.61	112.61	112.51	114.82	114.82	114.74	114.08	114.03	113.65
500	124.79	124.79	124.71	127.22	127.22	127.16	126.40	126.63	126.05
600	136.51	136.50	136.45	138.98	138.97	138.92	138.11	138.63	137.93
800	158.37	158.37	158.33	160.56	160.55	160.51	159.69	160.33	159.73
1000	178.12	178.12	178.09	179.83	179.82	179.78	179.01	179.73	179.33
1500	219.65	219.64	219.63	220.02	220.02	219.99	219.21		220.12
2000	252.66	252.65	252.64	251.84	251.83	251.81			
2400	274.67	274.67	274.66	273.02	273.01	272.99			

^a BMC-CCSD//M06-2X/MG3S. ^b CCSD(T)-F12a/jul-cc-pVTZ//M06-2X/MG3S. ^c Using Benson's data from ref. 13 and adding 0.026 cal mol⁻¹ K⁻¹ to convert from a standard pressure of 1 atm to a standard pressure of 1 bar. ^d Using API data from ref. 28 and adding 0.026 cal mol⁻¹ K⁻¹ to convert from a standard pressure of 1 atm to a standard pressure of 1 bar. ^e Using TRC data from ref. 29.

Table 8 Heat capacity of *n*-heptane in cal mol⁻¹ K⁻¹ at various temperatures

<i>T</i> (K)	MS-LH			MS-T			Benson ^c	Exp.-API ^d	Exp.-TRC ^e	Exp ^f
	M06-2X	BMC-CCSD ^a	CCSD(T)-F12a ^b	M06-2X	BMC-CCSD ^a	CCSD(T)-F12a ^b				
357.1	44.06	44.19	44.56	45.87	45.97	46.33	46.14			45.77
373.2	45.86	45.98	46.32	47.58	47.68	48.00	47.83			47.51
400.4	48.89	49.00	49.29	50.43	50.52	50.78	50.62			50.37
434.4	52.60	52.69	52.93	53.87	53.94	54.15	53.97			53.85
466.1	55.95	56.02	56.23	56.94	57.00	57.18	56.96			57.00
300	37.75	37.95	38.49	39.71	39.88	40.42	39.88	39.86	39.67	
400	48.85	48.95	49.25	50.39	50.48	50.74	50.43	50.42	50.36	
500	59.37	59.43	59.62	60.05	60.10	60.25	60.05	60.07	60.25	
600	68.49	68.53	68.67	68.28	68.32	68.41	68.33	68.33	68.69	
800	82.95	82.97	83.06	81.32	81.35	81.40	81.39	81.43	81.81	
1000	93.68	93.69	93.76	91.11	91.14	91.18	91.24	91.20	91.20	
1500	110.27	110.27	110.31	106.47	106.48	106.52	106.41	106.40	106.12	
2000	118.72	118.72	118.75	114.34	114.34	114.37				
2400	122.63	122.63	122.65	117.96	117.96	117.99				

^a BMC-CCSD//M06-2X/MG3S. ^b CCSD(T)-F12a/jul-cc-pVTZ//M06-2X/MG3S. ^c Using Benson's data from ref. 13. ^d Using API data from ref. 28. ^e Using TRC data from ref. 29. ^f The experimental data are from ref. 64.

a standard state of 1 atm, we correct them to a standard state of 1 bar in the present article; no such correction is needed for the values in the TRC tables, which already correspond to a standard state at 1 bar.)

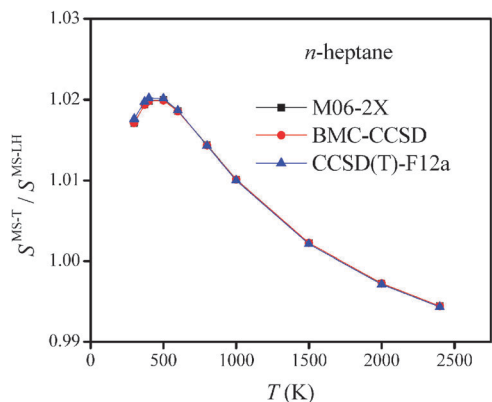
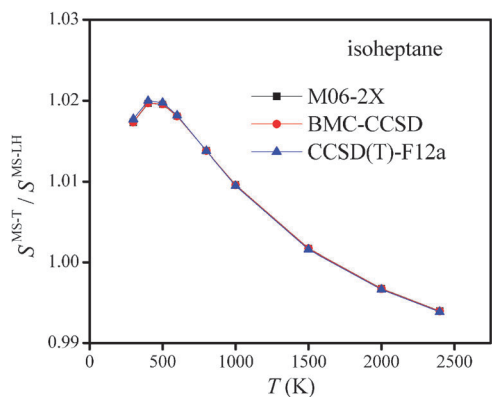
For both *n*-heptane and isoheptane in the temperature range from 298 K to 2400 K, as discussed above, the partition functions obtained by the MS-LH approximation are consistently smaller than those by MS-T. However, the calculated

Table 9 Heat capacity of isoheptane in $\text{cal mol}^{-1} \text{K}^{-1}$ at various temperatures

T (K)	MS-LH			MS-T			Benson ^c	Exp.-API ^d	Exp.-TRC ^e
	M06-2X	BMC-CCSD ^a	CCSD(T)-F12a ^b	M06-2X	BMC-CCSD ^a	CCSD(T)-F12a ^b			
300	38.56	38.51	38.74	40.40	40.35	40.28	39.61	39.86	39.32
400	49.52	49.49	49.62	50.90	50.87	50.98	50.37	50.42	50.67
500	59.85	59.84	59.93	60.42	60.40	60.46	60.12	60.07	60.66
600	68.83	68.83	68.90	68.55	68.55	68.59	68.47	68.33	69.19
800	83.11	83.12	83.18	81.47	81.46	81.49	81.58	81.43	82.60
1000	93.76	93.77	93.81	91.18	91.18	91.20	91.38	91.20	92.40
1500	110.28	110.28	110.31	106.46	106.47	106.48	106.66	106.40	108.03
2000	118.72	118.72	118.73	114.33	114.33	114.35			
2400	124.38	124.38	124.39	119.59	119.59	119.61			

^a BMC-CCSD//M06-2X/MG3S. ^b CCSD(T)-F12a/jul-cc-pVTZ//M06-2X/MG3S. ^c Using Benson's data from ref. 13. ^d Using API data from ref. 28. ^e Using TRC data from ref. 29.

entropies and heat capacities calculated using the MS-LH approximation are smaller than those obtained by MS-T in the low-temperature regime but larger in high-temperature regime. This observation can be explained by eqn (4), which shows that the entropy depends on the partition function and its temperature derivative. As a further consequence of this dependence, the ratio of the MS-T partition function to the MS-LH one is larger than the entropy ratio between MS-T and MS-LH results at each temperature (as shown in Fig. 9 and 10).

**Fig. 9** The ratio of entropies of *n*-heptane calculated by MS-T and MS-LH approximations at various temperatures.**Fig. 10** The ratio of entropies of isoheptane calculated by MS-T and MS-LH approximations at various temperatures.

Note that Benson's empirical parameters^{13,15} are based on the API tables, which are based on experimental data. The direct experimental measurement of the entropy of *n*-heptane by calorimetric method was accomplished by Pitzer at 371.5 K.⁶³ Waddington and Huffman⁶⁴ determined the heat capacity of *n*-heptane experimentally between 350 K and 470 K, and the heat capacity data at the other temperatures in the range from 298 K to 1500 K were calculated by Person and Pimental.⁶⁵ All of these results were used to generate the thermodynamic data in the API tables. Huffman *et al.*¹¹ determined the heat capacity isoheptane at low temperature in the liquid and solid state, and we did not find direct experimental measurements of the heat capacity in the gas phase in the temperature range from 298 K to 1500 K. The API tables recommend that the heat capacity of isoheptane should be assumed to be the same as *n*-heptane (our calculations confirm that this holds within $0.1 \text{ cal K}^{-1} \text{ mol}^{-1}$ for 300–2000 K), and entropy and other thermodynamic-data in the API tables for isoheptane are those estimated by Park *et al.* at 298 K.⁶⁶ The TRC tables are based on both direct measurements of thermodynamic properties and inferences from spectroscopic data.

For *n*-heptane, Table 8 demonstrates the heat capacity calculated by MS-T agrees well with the experimental values in the temperature range where they are available. At temperatures out of this range, MS-T calculations agree with Benson's estimates, with the TRC data series, and with the API data set very well. The entropy values we calculated using MS-T agree well with Pitzer's experimental data at 375.1 K, with the best results being obtained using CCSD(T)-F12a energies. At other temperatures between 298 and 1500 K, MS-T calculations with CCSD(T)-F12a energies are also consistent with Benson's estimates, the TRC data series, and the API data. Similarly, for the entropy and heat capacity of isoheptane, Table 7 and 9 show good agreement between the MS-T calculations and estimates based on Benson's data, the TRC data series, and the API data. All of these comparisons validate the MS-T method for predicting entropy and heat capacity.

Change of entropies, enthalpies, and free energies in the isomerization reaction between *n*-heptane and isoheptane

Using eqn (4)–(6), we obtain the entropy, enthalpy, and free energy for *n*-heptane and isoheptane and the change of entropies, enthalpies, and free energies in the isomerization reaction between

Table 10 Standard-state entropy, enthalpy, and free energy changes of the isomerization reaction between *n*-heptane and isoheptane

<i>T</i> (K)	MS-LH			MS-T			Benson ^c	Exp.-API ^d	Exp.-TRC ^e
	M06-2X	BMC-CCSD ^a	CCSD(T)-F12a ^b	M06-2X	BMC-CCSD ^a	CCSD(T)-F12a ^b			
ΔS° (cal/mol ⁻¹ K ⁻¹)									
298	-1.68	-1.58	-1.43	-1.68	-1.59	-1.44	-1.31	-1.89	-1.82
300	-1.67	-1.58	-1.34	-1.68	-1.58	-1.44	-1.31	-1.91	-1.82
400	-1.45	-1.41	-1.26	-1.50	-1.46	-1.38	-1.36	-1.42	-1.79
500	-1.33	-1.31	-1.21	-1.41	-1.38	-1.33	-1.36	-1.14	-1.70
600	-1.25	-1.24	-1.16	-1.35	-1.33	-1.29	-1.34	-0.79	-1.60
800	-1.18	-1.18	-1.14	-1.29	-1.28	-1.26	-1.28	-0.65	-1.51
1000	-1.15	-1.15	-1.13	-1.26	-1.26	-1.24	-1.25	-0.52	-1.20
1500	-1.14	-1.14	-1.13	-1.25	-1.26	-1.25	-1.19		-0.48
2000	-1.14	-1.14	-1.13	-1.26	-1.26	-1.26			
2400	-1.14	-1.14	-1.14	-1.26	-1.26	-1.26			
ΔH (kcal/mol)									
298	-1.53	-1.98	-1.60	-1.53	-1.98	-1.60	-2.40	-1.71	-1.63
300	-1.53	-1.98	-1.60	-1.53	-1.98	-1.60		-1.72	-1.63
400	-1.45	-1.92	-1.57	-1.47	-1.93	-1.58	-2.42	-1.59	-1.60
500	-1.39	-1.87	-1.53	-1.42	-1.90	-1.56	-2.42	-1.46	-1.58
600	-1.35	-1.84	-1.51	-1.39	-1.87	-1.54	-2.40	-1.27	-1.53
800	-1.31	-1.79	-1.47	-1.35	-1.84	-1.51	-2.37	-1.02	-1.39
1000	-1.28	-1.77	-1.46	-1.33	-1.82	-1.50	-2.34	-1.04	-1.20
1500	-1.26	-1.75	-1.45	-1.32	-1.82	-1.51	-2.27		-0.24
2000	-1.26	-1.75	-1.45	-1.33	-1.83	-1.52			
2400	-1.27	-1.76	-1.46	-1.33	-1.83	-1.53			
ΔG° (kcal/mol)									
298	-1.03	-1.51	-1.18	-1.03	-1.51	-1.17	-2.01	-1.15	-1.08
300	-1.03	-1.50	-1.17	-1.02	-1.50	-1.17		-1.15	-1.10
400	-0.87	-1.36	-1.03	-0.87	-1.35	-1.03	-1.87	-1.02	-0.91
500	-0.73	-1.22	-0.91	-0.72	-1.21	-0.89	-1.74	-0.89	-0.72
600	-0.60	-1.09	-0.78	-0.58	-1.07	-0.76	-1.60	-0.80	-0.57
800	-0.36	-0.85	-0.55	-0.32	-0.81	-0.51	-1.34	-0.50	-0.19
1000	-0.13	-0.62	-0.31	-0.07	-0.56	-0.26	-1.09	-0.52	0.02
1500	0.44	-0.05	0.25	0.56	0.07	0.36	-0.48		0.48
2000	1.01	0.52	0.81	1.19	0.70	0.99			
2400	1.47	0.98	1.27	1.69	1.20	1.49			

^a BMC-CCSD//M06-2X/MG3S. ^b CCSD(T)-F12a/jul-cc-pVTZ//M06-2X/MG3S. ^c For ΔS° , using Benson's data from ref. 13, For ΔH and ΔG° using Benson's data in ref. 15, which includes an updated heat formation data set comparing with those from ref. 13. ^d Using API data from ref. 28. ^e Using TRC data from ref. 29.

n-heptane and isoheptane. These results are shown in Table 10. The MS-T and MS-LH calculations agree well with each other at low temperature for ΔS° , ΔH , and ΔG° , but the deviations between the two approximation methods are larger in the high-temperature range, where the LH approximation breaks down.

Note that, our calculated data for the ΔS° results agree very well with estimations based on Benson's empirical data, and they are also close to the TRC data series and the API data set. For the ΔH results, Benson's method gives negative deviations compared with the API data; MS-LH and MS-T methods using M06-2X and CCSD(T)-F12a energies give positive deviations, and those using BMC-CCSD energies give negative deviations; but they all still agree with the API data set within ± 1 kcal/mol over the whole temperature range. A similar trend is observed for the ΔG° results.

Conclusions

In the present work, we applied the MS-T and MS-LH methods to calculate the partition functions for *n*-heptane and isoheptane. Furthermore, we used the partition functions to predict the thermodynamic quantities, such entropy and heat capacity, for these two species, and we also calculated ΔS° , ΔH , and ΔG° for the isomerization reaction between *n*-heptane

and isoheptane. The results show that all calculated thermodynamics quantities based on the MS-T method agree well with experimental data, in particular the API tables, the TRC data series, and estimates based on Benson's empirical parameters in the temperature range from 298 K to 1500 K. This shows that the MS-T method including both multi-structural anharmonicity and torsional anharmonicity effect can be used to calculate the thermodynamic properties for molecules containing many torsions. It also gives us confidence that we can extend the application of electronic structure theory with the MS-T method to predict the thermodynamic properties at even higher temperatures that are not included in the empirical API tables or TRC data series, and where empirical estimation would be a dangerous extrapolation, or—even more importantly for developing combustion mechanisms—to predict the thermodynamic parameters of many multiple-structure molecules where no data is available.

Acknowledgements

The authors are grateful to Steven Mielke and Wing Tsang for helpful suggestions. This work was supported by the U. S. Department of Energy, Office of Basic Energy Sciences under grant no. DE-FG02-86ER13579 and by the Combustion Energy Frontier Research Center under award no. DE-SC0001198.

References

- 1 K. S. Pitzer, *Chem. Rev.*, 1940, **27**, 39.
- 2 K. S. Pitzer and J. E. Kilpatrick, *Chem. Rev.*, 1946, **39**, 435.
- 3 J. F. Messerly, G. B. Guthrie, S. S. Todd and H. L. Finke, *J. Chem. Eng. Data*, 1967, **12**, 338.
- 4 J. F. Messerly, S. S. Todd and H. L. Finke, *J. Phys. Chem.*, 1965, **69**, 353.
- 5 H. L. Finke, J. F. Messerly and S. S. Todd, *J. Phys. Chem.*, 1965, **69**, 2094.
- 6 J. F. Messerly, S. S. Todd and H. L. Finke, *J. Phys. Chem.*, 1965, **69**, 4304.
- 7 D. W. Scott, In *Chemical Thermodynamic Properties of Hydrocarbons and Related Substances. Properties of the Alkane Hydrocarbons, C1 through C10 in the Ideal Gas State from 0 to 1500 K*, U. S. Bureau of Mines, Bulletin 666, 1974.
- 8 J. B. Green Shields and F. D. Rossini, *J. Phys. Chem.*, 1958, **62**, 271.
- 9 G. B. Guthrie Jr. and H. M. Huffman, *J. Am. Chem. Soc.*, 1943, **65**, 1139.
- 10 D. R. Douslin and H. M. Huffman, *J. Am. Chem. Soc.*, 1946, **68**, 1704.
- 11 H. M. Huffman, M. E. Gross, D. W. Scott and J. P. McCullough, *J. Phys. Chem.*, 1961, **65**, 495.
- 12 D. W. Scott, G. Waddington, J. C. Smith and H. M. Huffman, *J. Chem. Phys.*, 1947, **15**, 565.
- 13 S. W. Benson, in *Thermochemical Kinetics*, Wiley-Interscience, New York, 2nd edn 1976.
- 14 H. E. O'Neal and S. W. Benson, *Int. J. Chem. Kinet.*, 1969, **1**, 221.
- 15 N. Cohen and S. W. Benson, *Chem. Rev.*, 1993, **93**, 2419.
- 16 S. W. Benson and J. H. Buss, *J. Chem. Phys.*, 1958, **29**, 546.
- 17 K. S. Pitzer and W. D. Gwinn, *J. Chem. Phys.*, 1942, **10**, 428.
- 18 (a) D. G. Truhlar, *J. Comput. Chem.*, 1991, **12**, 266; (b) Y.-Y. Chuang and D. G. Truhlar, *J. Chem. Phys.*, 2000, **112**, 1221. [errata: 2004, **121**, 7036; 2006, **125**, 179903]; (c) B. A. Ellingson, V. A. Lynch, S. L. Mielke and D. G. Truhlar, *J. Chem. Phys.*, 2006, **125**, 84305.
- 19 B. M. Wong and W. H. Green, *Mol. Phys.*, 2005, **103**, 1027.
- 20 P. Vansteenkiste, D. V. Neck, V. Van Speybroeck and M. Waroquier, *J. Chem. Phys.*, 2006, **124**, 044314; P. Vansteenkiste, T. Verstraelen, V. Van Speybroeck and M. Waroquier, *Chem. Phys.*, 2006, **328**, 251.
- 21 D. Gruzman, A. Karton and J. M. L. Martin, *J. Phys. Chem. A*, 2009, **113**, 11974.
- 22 J. Zheng, T. Yu, E. Papajak, I. M. Alecu, S. L. Mielke and D. G. Truhlar, *Phys. Chem. Chem. Phys.*, 2011, **13**, 10885.
- 23 T. Yu, J. Zheng and D. G. Truhlar, *Chem. Sci.*, 2011, **2**, 2199.
- 24 J. Zheng, T. Yu and D. G. Truhlar, *Phys. Chem. Chem. Phys.*, 2011, DOI: 10.1039/C1CP21829H.
- 25 B. M. Wong and S. Raman, *J. Comput. Chem.*, 2007, **28**, 759.
- 26 B. M. Wong, M. M. Fadri and S. Raman, *J. Comput. Chem.*, 2008, **29**, 481.
- 27 D. P. Tew, N. C. Handy, S. Carter, S. Irlé and J. M. Bowman, *Mol. Phys.*, 2003, **101**, 3513.
- 28 API Tables: *Selected Values of Properties of Hydrocarbons and Related Compounds*, American Petroleum Institute Research Project 44, Carnegie Press (Carnegie Institute of Technology), Pittsburgh, PA, 1953.
- 29 TRC Data Series: M. Frenkel, G. J. Kabo, K. N. Marsh, G. N. Roganov and R. C. Wilhoit, *Thermodynamics of Organic Compounds in the Gas State*, CRC Press, Boca Raton, FL, vol. II, 1994.
- 30 I. M. Alecu, J. Zheng, Y. Zhao and D. G. Truhlar, *J. Chem. Theory Comput.*, 2010, **6**, 2872.
- 31 D. G. Truhlar and A. D. Isaacson, *J. Chem. Phys.*, 1991, **94**, 357.
- 32 B. C. Garrett and D. G. Truhlar, *J. Phys. Chem.*, 1979, **83**, 1915.
- 33 A. D. Isaacson, D. G. Truhlar, K. Scanlon and J. Overend, *J. Chem. Phys.*, 1981, **75**, 3017.
- 34 Y. Zhao and D. G. Truhlar, *Theor. Chem. Acc.*, 2007, **120**, 215.
- 35 (a) R. Krishnan, J. S. Binkley, R. Seeger and J. A. Pople, *J. Chem. Phys.*, 1980, **72**, 650; (b) T. Clark, J. Chandrasekhar, G. W. Spitznagel and P. v. R. Schleyer, *J. Comput. Chem.*, 1983, **4**, 294; (c) M. J. Frisch, J. A. Pople and J. S. Binkley, *J. Chem. Phys.*, 1984, **80**, 3265.
- 36 B. J. Lynch, Y. Zhao and D. G. Truhlar, *J. Phys. Chem. A*, 2003, **107**, 1384.
- 37 B. J. Lynch, Y. Zhao and D. G. Truhlar, *J. Phys. Chem. A*, 2005, **109**, 1643.
- 38 T. B. Adler, G. Knizia and H.-J. Werner, *J. Chem. Phys.*, 2007, **127**, 221106.
- 39 G. Knizia, T. B. Adler and H.-J. Werner, *J. Chem. Phys.*, 2009, **130**, 054104.
- 40 (a) E. Papajak and D. G. Truhlar, *J. Chem. Theory Comput.*, 2011, **7**, 10; (b) E. Papajak and D. G. Truhlar, *J. Chem. Theory Comput.*, 2010, **6**, 597.
- 41 M. J. Frisch, G. W. Trucks, H. B. Schlegel, G. E. Scuseria, M. A. Robb, J. R. Cheeseman, G. Scalmani, V. Barone, B. Mennucci, G. A. Petersson, H. Nakatsuji, M. Caricato, X. Li, H. P. Hratchian, A. F. Izmaylov, J. Bloino, G. Zheng, J. L. Sonnenberg, M. Hada, M. Ehara, K. Toyota, R. Fukuda, J. Hasegawa, M. Ishida, T. Nakajima, Y. Honda, O. Kitao, H. Nakai, T. Vreven Jr., J. A. Montgomery, J. E. Peralta, F. Ogliaro, M. Bearpark, J. J. Heyd, E. Brothers, K. N. Kudin, V. N. Staroverov, R. Kobayashi, J. Normand, K. Raghavachari, A. Rendell, J. C. Burant, S. S. Iyengar, J. Tomasi, M. Cossi, N. Rega, N. J. Millam, M. Klene, J. E. Knox, J. B. Cross, V. Bakken, C. Adamo, J. Jaramillo, R. Gomperts, R. E. Stratmann, O. Yazyev, A. J. Austin, R. Cammi, C. Pomelli, J. W. Ochterski, R. L. Martin, K. Morokuma, V. G. Zakrzewski, G. A. Voth, P. Salvador, J. J. Dannenberg, S. Dapprich, A. D. Daniels, Ö. Farkas, J. B. Foresman, J. V. Ortiz, J. Cioslowski and D. J. Fox, *Gaussian 09, Revision A.02*, Gaussian, Inc., Wallingford CT, 2009.
- 42 Y. Zhao and D. G. Truhlar, *MLGAUSS computer program, version 2.0*, University of Minnesota, Minneapolis, 2007.
- 43 H.-J. Werner, P. J. Knowles, F. R. Manby, M. Schütz, P. Celani, G. Knizia, T. Korona, R. Lindh, A. Mitrushenkov, G. Rauhut, T. B. Adler, R. D. Amos, A. Bernhardsson, A. Berning, D. L. Cooper, M. J. O. Deegan, A. J. Dobbyn, F. Eckert, E. Goll, C. Hampel, A. Hesselmann, G. Hetzer, T. Hrenar, G. Jansen, C. Köppl, Y. Liu, A. W. Lloyd, R. A. Mata, A. J. May, S. J. McNicholas, W. Meyer, M. E. Mura, A. Nicklaß, P. Palmieri, K. Pflüger, R. Pitzer, M. Reiher, T. Shiozaki, H. Stoll, A. J. Stone, R. Tarroni, T. Thorsteinsson, M. Wang, A. Wolf, *Molpro*, University of Birmingham, Birmingham, 2010.1, 2010.
- 44 J. Zheng, S. L. Mielke, K. L. Clarkson and D. G. Truhlar, *MSTOR computer program, version 2011*, University of Minnesota, Minneapolis, 2011.
- 45 C. J. Hoeve, *J. Chem. Phys.*, 1961, **35**, 1266.
- 46 K. Naqai and T. Ishikawa, *J. Chem. Phys.*, 1962, **37**, 496.
- 47 P. J. Flory and R. L. Jernigan, *J. Chem. Phys.*, 1965, **42**, 3509.
- 48 K. S. Pitzer, *J. Chem. Phys.*, 1940, **8**, 711.
- 49 R. A. Scott and H. A. Scheraga, *J. Chem. Phys.*, 1966, **44**, 3054.
- 50 R. D. Burkhart and J. C. Merrill, *J. Chem. Phys.*, 1967, **46**, 4985.
- 51 K. Nagai, *J. Chem. Phys.*, 1968, **48**, 5646.
- 52 T. Yasukawa and C. Chachaty, *Chem. Phys. Lett.*, 1976, **43**, 565.
- 53 B. Tevlin, S. Laffleur and L. E. H. Trainon, *Chem. Phys. Lett.*, 1985, **122**, 581.
- 54 S. Tsuzuki, L. Schlifer, H. Goto, E. D. Jemmis, H. Hosoya, K. Siam, K. Tanabe and E. Osawa, *J. Am. Chem. Soc.*, 1991, **113**, 4665.
- 55 H. Goto, E. Osawa and M. Yamato, *Tetrahedron*, 1993, **49**, 387.
- 56 R. L. Dunbrack, Jr. and M. Karplus, *Nat. Struct. Biol.*, 1994, **1**, 334.
- 57 G. Tasi, F. Mizukami, I. Pálíncó, J. Csontos, W. Györfy, P. Nair, K. Maeda, M. Toba, S.-i. Niwa, Y. Kiyozumi and I. Kiricsi, *J. Phys. Chem. A*, 1998, **102**, 7698.
- 58 R. Y. Dong, *Phys. Rev. E: Stat. Phys., Plasmas, Fluids, Relat. Interdiscip. Top.*, 1999, **60**, 5631.
- 59 T. M. Madkoun and A. Soldera, *Eur. Polym. J.*, 2001, **37**, 1105.
- 60 J. B. Klauda, B. R. Brooks, A. D. Mackerell, R. M. Venable and R. W. Pastor, *J. Phys. Chem. B*, 2005, **109**, 5300.
- 61 J. B. Klauda, R. W. Pastor and B. R. Brooks, *J. Phys. Chem. B*, 2005, **109**, 15684.
- 62 W. L. Mattice, N. Waheed and F. Ergüney, *Macromol. Theory Simul.*, 2006, **15**, 529.
- 63 K. S. Pitzer, *J. Am. Chem. Soc.*, 1940, **62**, 1224.
- 64 G. Waddington, S. S. Todd and H. M. Huffman, *J. Am. Chem. Soc.*, 1947, **69**, 22.
- 65 W. B. Person and G. C. Pimentel, *J. Am. Chem. Soc.*, 1953, **75**, 532.
- 66 G. S. Parks, H. M. Huffman and S. B. Thomas, *J. Am. Chem. Soc.*, 1930, **52**, 1032.